IEEE Access
Multidisciplinary | Rapid Review | Open Access Journal

Received August 19, 2021, accepted September 18, 2021, date of publication September 23, 2021, date of current version October 5, 2021.

Digital Object Identifier 10.1109/ACCESS.2021.3115337

Implementation and Evaluation of Novel Architecture Using Optical Wireless for WLAN Control Plane

RYOTA SHIINA[1], SHINYA TAMAKI[1], KAZUTAKA HARA[1], TOMOHIRO TANIGUCHI[1], SHUNSUKE SARUWATARI[2], (Member, IEEE), AND TAKASHI WATANABE[2], (Member, IEEE)

[1]NTT Access Network Service Systems Laboratories, NTT Corporation, Tokyo 180-8585, Japan
[2]Graduate School of Engineering, Osaka University, Osaka 565-0871, Japan

Corresponding author: Ryota Shiina (ryota.shiina.ys@hco.ntt.co.jp)

ABSTRACT We propose a novel wireless control system architecture that divides the wireless service area into smaller optical cells and centrally controls the user equipment (UE) connections under each optical cell. The proposal transmits via IoT smart lighting an optical identifier (ID) specifying connection information to the UE with illuminance sensor. The received optical ID indicates the optimum connection destination. Two solutions are proposed to overcome the hardware restrictions faced by optical ID transmission/reception. Oversampled edge-excluded receiving scheme (OE) reduces the error rate; the signal is oversampled and each window subjected to majority decision. Optical ID reception with lower error rate than conventional approach is realized with a minimum received illuminance of just 8.5 lx (background illuminance 226.67 lx) and a modulation factor of 7 %. Fast optical ID authentication (FA) reduces the authentication cycle preceding optical ID reception by performing correlation calculation between the cyclic matrix and an optical ID list. FA shortens the authentication cycle by 62.5 % (1200 ms to 450 ms). Furthermore, an optical cell control algorithm (ScanLine-based/MinDist-based) is proposed to offset the deterioration in network quality created by non-uniform UE distribution. ScanLine-based algorithm controls optical cells in scanning line manner, while MinDist-based favors optical cells with the minimum distance from the access point (AP). It is confirmed that with an optical cell radius of 5 m or less, the capacity difference per user is reduced compared to the existing RSSI-based alternative while reducing the deterioration of total capacity in extremely biased user distribution scenarios.

INDEX TERMS Wireless local area network hotspot, optical wireless communication, optical cell operation, wireless local area network control plane.

I. INTRODUCTION

The demand for wireless communication has been remarkable in recent years, and the use of user equipment (UE) has exploded [1]. By 2022, wired networks will account for 29.4 % of Internet protocol (IP) traffic, and Wi-Fi devices and mobile networks will account for 70.6 % of that traffic [1]. Wireless services have made it possible for everyone to connect to the network. In particular, wireless local area network (WLAN) services based on IEEE 802.11 are widely deployed in public facilities and commercial facilities, and many hotspots have been deployed [2]. Hotspots are now being offered as a value-added service to commercial services [3]. In other words, network service is being provided as a commercial tool for the purpose of attracting customers. However, if the quality of the communication environment provided is problematic, customer satisfaction with the entire commercial service may be degraded [4]–[6]. Therefore, the quality and convenience of the communication environment is a critical factor.

However, hotspot services have challenges in terms of providing access only to UEs in the target area and service quality. Existing services are not able to provide location-aware hotspots. With existing systems, it is difficult to provide network connection to just the UEs in a specific region within the wireless access area. In other words, it is difficult

The associate editor coordinating the review of this manuscript and approving it for publication was Xujie Li.

to limit the usage area based on location [7]. This means that there is a lack of flexibility in the provision of hotspot services. Furthermore, there is a possibility of unintended network access from outside the target area. This is because, due to the diffraction property of wireless signals, it is physically possible to communicate beyond the target area. Such unintended use of the network can degrade the communication quality as perceived by the primary target users. This may induce a decrease in customer satisfaction with the entire commercial service. Network access restriction is generally achieved by distributing different passwords to the UEs to differentiate the target areas, but there is a concern that this will reduce usability [8].

Additionally, from the network provisioning viewpoint, existing received signal strength indicator (RSSI)-based systems have difficulty in load balancing with fine granularity, and the network quality fluctuates according to UE distribution [9]. In existing systems, it is difficult to control UE connections according to the individual UE location. For example, a UE connects to the access point (AP) with the strongest RSSI when it first connects. However, as the UE moves and its location changes, the throughput deteriorates [10]. The distribution of UEs is rarely spatially uniform, and congestion often occurs in different areas. Depending on distribution irregularity, network quality can be significantly degraded [9]. Furthermore, highly irregular UE distributions can generate excessive network traffic concentration on individual APs [11].

Various approaches have been proposed to support non-uniform distributions of UEs. One approach is for each UE to make its own AP selection decisions depending on their state. Each UE calculates the optimal AP by itself and connects to the destination under its own initiative. The second approach is to collect network information from a central AP or controller and then determine the connection destination for each UE based on that information. In this approach, network parameters including RSSI between UE and AP are used to determine the connection destination. However, in an environment where a large number of UEs and an extremely concentrated user distribution occur, it is difficult to perform fine-grained connection control, so an approach that considers the absolute UE position is also being considered. In order to improve the accuracy of UE position determination, one approach utilizes not only the radio waves themselves but also other media. By utilizing such position determination, it is possible to calculate the optimum connection destination. Unfortunately, this approach makes it necessary to modify UE hardware and software to add the functions needed.

In order to realize location-aware service provisioning and fine-grained network control in hotspot services, we propose a new wireless control system architecture that intentionally divides the wireless service area into small optical cells and controls the connection of UEs in each optical cell. In the proposed system, optical identifiers (IDs) that represent network connection information are distributed to each optical cell, authentication and connection are performed according to the optical IDs, and AP assignment can be dynamically changed by changing the optical ID. In our proposal, we limit the network available area by performing location-based authentication for each optical cell. In addition, by coordinating optical cells, it is possible to set up partially available/unavailable areas within the radio wave coverage area, and flexible authentication and connection can be easily realized. Instead of using a built-in dedicated optical wireless transceiver, smart light emitting diode (LED) lighting is used as the ID light source, and the illumination sensors or cameras in existing smartphones are used to receive optical IDs. Therefore, the system can be realized without modifying existing UE hardware, thereby reducing the barriers to implementation.

To further improve the benefits of the proposed system in terms of network quality, we propose an optical cell control algorithm that guarantees high network quality against temporal variations in UE location distribution. In this algorithm, UE connection control is performed by considering the traffic of each AP and the absolute location of the optical cells and APs, without actively collecting UE location information. We show that our proposal enables load balancing among APs while ensuring fairness of capacity among UEs under each AP in various UE location distribution scenarios. We also show that, by considering the location of each AP and optical cell, the total system capacity reduction caused by load balancing among APs can be minimized.

Section II describes relevant studies in the literature. Section III describes the entire proposal. First, we describe the architectural details and configuration, and propose an optical ID distribution scheme. In addition, we also propose an optical cell control algorithm. Section IV shows the results of a field evaluation of the optical ID distribution scheme and the scenario-based evaluation of the effectiveness of the proposed architecture under various UE distributions. We also discuss the design of the optical cell. Section V summarizes this work.

The contributions of this paper are as follows.

- Proposal of an WLAN control architecture that divides the network service area by optical cells and realizes flexible but simple connection control for each optical cell.
- Experimental evaluation of the proposed optical ID transmission/reception scheme by implementing the architecture with general IoT lighting and the illuminance sensors installed in smartphones.
- Evaluation of the proposed optical cell control algorithm that achieves fairness and high average capacity against local UE concentration and fluctuation in user distribution.

II. RELATED WORKS

This section describes related works on AP connection selection and location estimation.

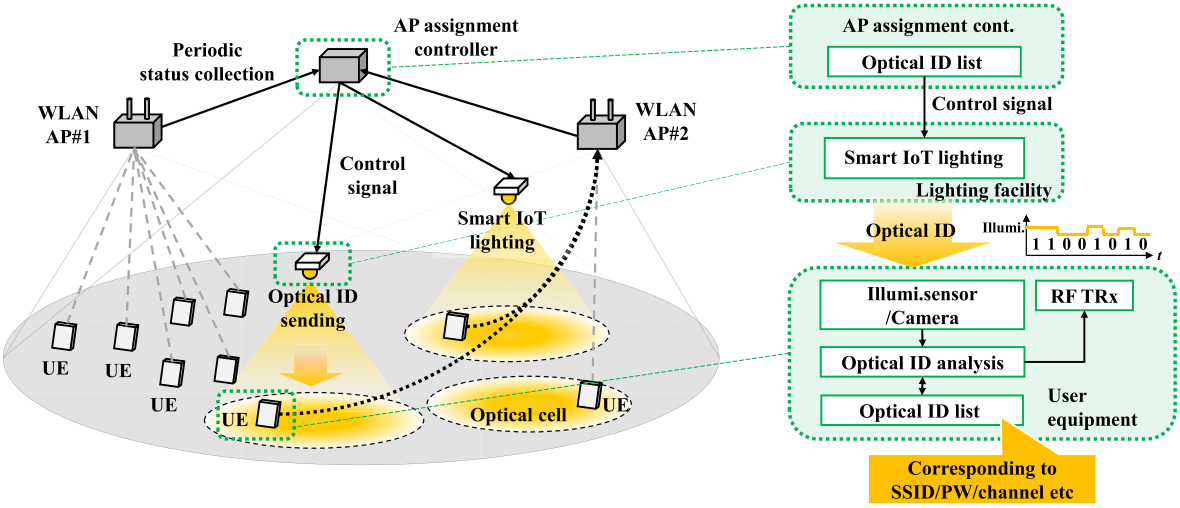

FIGURE 1. Proposed system architecture that applies optical wireless to the control plane of WLAN.

A. RESEARCH RELATED TO ACCESS POINT SELECTION

Various techniques have been proposed for AP assignment. They can be roughly divided into two types: UE-driven and network-driven.

The UE-driven type has the UE select and connect to an AP. In existing WLAN systems, the UE takes the initiative in connecting to the AP with the strongest RSSI among connectable APs [12]. An alternative method uses the round trip time (RTT) between the UE and AP to trigger connection switching [13]. In [14], the UE selects the connection destination AP by itself according to the moving direction of the UE by using the geomagnetic sensor set in the UE. All of these UE-driven type methods tend to optimize the individual connection quality via RSSI.

On the other hand, network-driven type methods assess the entire network and distribute UE connections from the viewpoint of network resources. The AP and controller basically perform centralized connection control based on the collected UE information. For example, one method changes the physical locations of the access points based on the information of UE location distribution. Dynamically changing AP placement is expected to improve the communication quality adaptively, even if the UE distribution fluctuates [15], [16]. However, the APs need to be equipped with a mobility mechanism. An alternative dynamically changes the transmission power according to UE location. These so-called cell-breathing methods control the transmission power of the AP, and a UE experiencing weak RSSI is forcibly reconnected to another AP [17], [18]. In the cell-breathing scheme, the control granularity of UEs to be load balanced is limited, and fine-grained connection control is difficult.

There are also several load balancing schemes for the AP side based on parameters that can be collected at each AP. The main parameter collected is the number of active UEs [19]. In addition to the number of UEs, [20] also considers the RSSI between the UE and the AP. Furthermore, in [21], the data rate is also employed as a parameter along with RSSI. However, in these RSSI-based schemes, the uncertainty in RSSI determination makes it difficult to select the correct UE for balancing in environments where the number of UEs is extremely high or they are unevenly distributed. Hence, throughput bias among UEs or APs will occur.

In addition to the relevant parameters mentioned above, a method has been proposed that uses the geographic location of the UE for connection selection. In [22], the location information of UEs is estimated from the RSSI of beacons and a distribution map is created, which is then used to select the connection destination. This is based on the RSSI of the beacons. It is affected by uncertainty in environments where the distribution is skewed. Reference [23] proposed a method that uses deep learning to estimate UE location from the radio signal (radio parameters other than RSSI) to achieve advanced location awareness and use location results for AP selection. However, achieving accurate location estimation incurs heavy computation costs. This problem worsens as UE number increases.

B. LOCATION ESTIMATION SCHEME

Various studies have been conducted to estimate the location of UEs. In addition, services related to location information have been actively proposed. The global positioning system (GPS) is well known as a source of location information [24]. Although GPS can determine location with high accuracy when used outdoors, it is well known that its accuracy is poor indoors.

An indoor positioning technique that uses sound waves has been proposed [25], [26]. This can estimate the position in three dimensions. There is also a positioning technique that uses the channel characteristics of wireless signals [27], [28]. References [27], [28] proposed a position estimation technique using channel state information (CSI). It has been reported that using CSI improves the accuracy of position

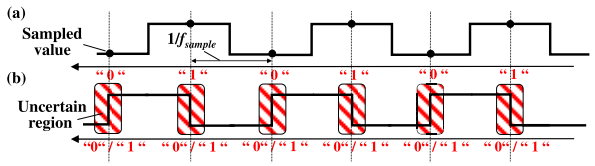

FIGURE 2. Reception error in asynchronous correlation receiving scheme.

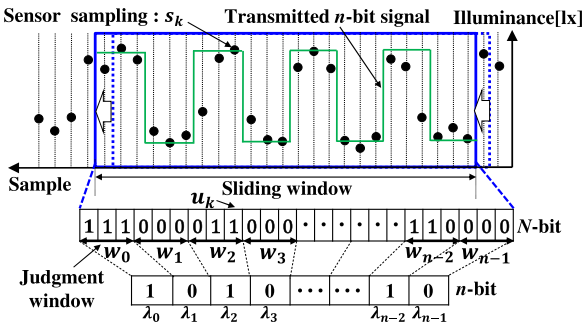

FIGURE 3. Detailed understanding of the oversampled edge-excluded receiving scheme (OE).

estimation compared to using RSSI. Unfortunately, these proposals require the use of special devices dedicated as transmitters and receivers. To ensure convenience and practicality in implementing area-based connection restriction in hotspots, it is desirable to use an approach that does not use special devices and does not involve UE modification.

III. PROPOSAL: OPTICAL WIRELESS FOR WLAN CONTROL PLANE

A. PROPOSED SYSTEM ARCHITECTURE

1) OVERALL ARCHITECTUE

Figure 1 shows the proposed system architecture. We assume a hotspot service with multiple APs that overlap each other. In addition, we also assume that there are multiple optical cells with smaller areas in the WLAN area. Specifically, the optical cells are created by smart Internet of Things (IoT) lighting using LEDs that can be dimmed by external control. The smart IoT lighting is used as an array of optical wireless transmitters; the modulation level is so low that it cannot be perceived by humans, and its lighting function is retained.

In our system architecture, AP selection is centrally controlled for each optical cell. The optical cells distribute the optical IDs, which are used for authentication and connection control. By knowing the installation location of the optical cell in advance, we can flexibly establish permitted and restricted areas. In addition, location-based connection control, which utilizes the installation location of optical cells, is expected to effectively realize load balancing, even when UEs move their locations or crowd together. The mechanism of connection control by optical cells and its flow are shown below.

In our system architecture, APs and smart IoT lighting are connected to a central AP assignment controller in a basic star network topology. The status of UEs under each AP is managed, and the connection status is periodically collected from APs by the central AP assignment controller. Here, the status indicates information related to WLAN such as the number of UEs, channels, and frequencies of each AP. Based on this status, the optical ID is determined by the AP assignment controller for each optical cell. Here, the optical ID is an arbitrary orthogonal bit sequence. Individual bit sequences are associated with individual SSID/PW. Optical IDs can be operated locally rather than globally to reduce the bit length. For example, in a small area such as the wireless service area of a commercial facility, about 8-bits is sufficient. A control signal for modulating the determined optical ID is sent from the AP assignment controller to the light source. The optical ID is broadcast to the UE in the optical cell. By transmitting the optical ID, the transmission rate required is reduced compared to sending the SSID/PW directly, making it possible to utilize IoT lighting with lower modulation facto and illuminance sensors with lower sampling rates as transmitters and receivers (TRx). The UE that receives an optical ID refers to an optical ID list loaded in advance and tries to connect to the specified AP. Here, the optical ID list associates the optical ID with connection information (i.e. SSID/PW etc.,). After receiving the optical ID, the UE makes the connection specified by the authentication process.

Instead of a dedicated optical wireless transceiver, we utilize general IoT lighting as the transmitter and a smartphone's illuminance sensor as the receiver. The advantage of the proposed system is that it is expected to become widespread given the rapid penetration of IoT. For example, the spread of IoT lighting systems is expected to increase more and more for the purpose of energy saving [29]–[32]. However, there are trade-offs due to the use of general IoT equipment. One is that it is difficult to increase the transmission speed. Due to the limited speed of IoT lighting modulation and the sampling frequency of most illumination sensors, the amount of information that can be transmitted is limited. This makes it difficult to insert the synchronous bits. As a result, it becomes difficult to achieve low error communication. In the next section, we detail our optical ID-based transmission/reception method that overcomes these problems. Another issue with our proposal is that the AP assignment controller and the UEs need to have a common optical ID list in advance. Our system enables UE control even at low speeds by maintaining an optical ID list that contains the optical IDs corresponding to the information to be transmitted. Considering these points, TRx must be economical and convenient in order to break down the hurdles of system diffusion and implementation, so it should be possible to use existing devices and smartphones without modification.

2) OPTICAL ID TRANSMISSION AND RECEPTION SCHEME USING CONSUMER SMART IOT LIGHTING AND SMARTPHONES

In order to improve the economy and convenience of sending and receiving optical IDs, existing lighting and smartphones must be used instead of dedicated optical

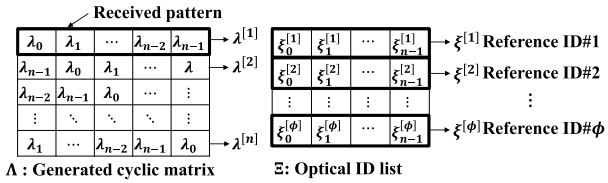

FIGURE 4. Generated cyclic matrix and optical ID list.

transmission/reception devices such as Light-Fidelity (Li-Fi) [33]. In addition, the optical ID receivers must be implemented as a simple smartphone application. Therefore, we propose an optical ID transmission and reception scheme to utilize IoT smart lighting as the transmitter, and the illuminance sensor of the smartphone as the receiver.

However, there are several technical issues. First, the transmission speed depends on the sampling frequency of the TRx, which is extremely low. Since it is difficult to use synchronous bits such as preambles, asynchronous communication must be used, resulting in high error rates. Also, due to the limited transmission speed, it takes time to receive and authenticate the optical ID.

One well known pattern matching method is that used in an intelligent lighting system [34]. This approach has the advantage of simplicity as optical correlation receiving is used. As shown in Fig. 2(a), there is no reception error when sampling is performed at the correct position for the received pulse. However, in the case of asynchronous communication, as shown in Fig. 2(b), errors are likely to occur when sampling is performed in an uncertain region, such as at the rising/falling edge of a pulse, where 1/0 judgment is uncertain. To address this issue, we propose an oversampled edge-excluded receiving scheme (OE). OE makes it possible to ignore uncertain regions (the edges) that hinder ID determination. OE can estimate the optical ID by oversampling the transmitted n-bit signal and performing window-based decision for each defined window length. Fig. 3 details the proposed receiving process. The received illuminance is binarized using a threshold value calculated from the average illuminance value in the sliding window. OE uses this sliding window to extract oversampled N-bit arrays. Here, signal u_k after binarization is represented by the following equation.

$$u_k = \begin{cases} 1 & \text{if } s_k \geq \dfrac{\sum_{l=1}^{l=N} s_{k-N+l}}{N} \\ 0 & \text{if } s_k < \dfrac{\sum_{l=1}^{l=N} s_{k-N+l}}{N} \end{cases} \tag{1}$$

Here, s_k represents the sensor sampling instances in the sliding window; sliding window length for binarization is N. The binarized N-bit signal is converted into an n-bit optical ID by using a judgement window. λ_k, which constitutes the optical ID after window-based judgement, is given by the following equation.

$$\lambda_k = \begin{cases} 1 & \text{if } sum\{w_k\} > \dfrac{K}{2} \\ 0 & \text{if } sum\{w_k\} \leq \dfrac{K}{2} \end{cases} \tag{2}$$

Here, the window length for window-based is, for the k-th judgement window, set to K $(= N/n)$. By performing these processes at the UE, uncertain regions (the edges) of the transmitted signal that hinder the determination of optical ID can be avoided, and the error rate can be reduced even with asynchronous signaling.

In the OE proposal described in advance, oversampling is performed K times compared to the existing receiving method. This means that the matching cycle between the received optical ID and the reference ID is also K times longer. A matching cycle is represented by the following equation.

$$T_{periodic} = K \cdot n \cdot 1/f_{sample} \tag{3}$$

n is the number of bits of the optical ID, and f_{sample} indicates the sampling frequency of the illuminance sensor. $T_{periodic}$ increases in proportion to n and K. The $T_{periodic}$ indicates the shortest period during which optical ID can be pattern matched. Therefore, in order to ensure usability, it is necessary to reduce $T_{periodic}$ as much as possible. Therefore, we also propose a fast optical ID authentication scheme (FA) that reduces the authentication cycle. The proposed method compares not only the optical ID itself, but also n bit-shifted patterns of the optical ID and the reference ID on the optical ID list in each sampling cycle. The optical ID is given by

$$\Lambda_{received} = \begin{bmatrix} \lambda_0 & \lambda_1 & \cdots & \lambda_{n-2} & \lambda_{n-1} \end{bmatrix}. \tag{4}$$

As shown in Fig. 4, cyclic matrix Λ is generated by bit-shifting the received optical ID. The optical ID list Ξ is prepared in advance. Here, ϕ indicates the number of reference IDs in optical ID list, and $\xi^{[\phi]}$ indicates the reference ID#ϕ. The k row of the cyclic matrix (i.e. $\lambda^{[k]}$) and the j row of the optical ID list (i.e. $\xi^{[j]}$) are extracted, and the correlation coefficient $\gamma_{\lambda^{[k]}\xi^{[j]}}$ is calculated by the following equation.

$$\gamma_{\lambda^{[k]}\xi^{[j]}} = \frac{\frac{1}{n}\sum_{i=0}^{n-1}\left(\lambda_i^{[k]} - \lambda^{\bar{[k]}}\right)\left(\xi_i^{[j]} - \xi^{\bar{[j]}}\right)}{\sqrt{\frac{1}{n}\sum_{i=0}^{n-1}\left(\lambda_i^{[k]} - \lambda^{\bar{[k]}}\right)^2} \cdot \sqrt{\frac{1}{n}\sum_{i=0}^{n-1}\left(\xi_i^{[j]} - \xi^{\bar{[j]}}\right)^2}} \tag{5}$$

The correlation coefficient between each row in the cyclic matrix and each row in the optical ID list (i.e. reference ID) is calculated by in round-robin manner. The reference ID#j with the highest correlation coefficient is determined by using following equation.

$$\xi^{[j]} = \arg \max_{\substack{k,f,\in\mathbb{N} \\ 1\leq k\leq n \\ 1\leq j\leq \phi}} \left\{\gamma_{\lambda^{[k]}\xi^{[j]}}\right\} \tag{6}$$

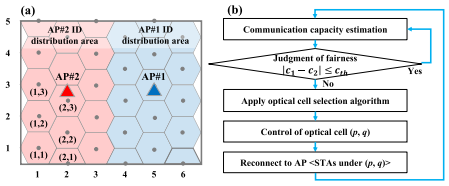

FIGURE 5. Optical cell operation framework. (a) Arrangement and configuration of AP and optical cell. (b) Overall flow chart of optical cell operation.

Finally, the reference ID#j corresponding to the received optical ID is extracted from the optical ID list. The matching cycle when FA is applied to the OE is expressed by using sampling frequency of illuminance sensor f_{sample}.

$$T_{periodic\_FA} = K \cdot 1/f_{sample} \tag{7}$$

Matching cycle duration can be reduced by the factor of n compared to when only OE is used.

These processes can be implemented in software and run on the UE.

B. OPTICAL CELL OPERATION POLICY

The proposed architecture controls the optical ID distributed in each optical cell based on UE connection state. Our cell operating objective is to reduce the excessive network load on individual APs (i.e. bias of traffic among APs) and the unfairness among UEs under different APs, caused by UE mobility and local clusters. Therefore, optical cell control is based on the following policy.

- Reduce the difference in average capacity per UE among the APs.
- Reduce the network load bias of each AP

To satisfy the above policy, the optical ID sent to each optical cell is determined based on the algorithm described below.

Figure 5 shows the framework for optical cell control. In the framework, a threshold based on fairness is first defined. Until the threshold is satisfied, the following operations are repeated: select an optical cell in the order given by the algorithm described below, changing the optical ID to be delivered, and switching the AP to which the UE is connected. As shown in Fig 5. (a), we assume that two APs, AP#1 and AP#2, are deployed in a wireless service area hosting a large number of UEs. The placement coordinates (x, y) of the visible light source and the placement coordinates of AP#1 and AP#2 are known in advance. Fig 5. (b) shows the flow of optical cell control. First, estimate the average capacity per UE for AP#1 and for AP#2 based on the traffic and number of UEs for each AP. If the following is satisfied, monitoring is continued.

$$|c_1 - c_2| \le c_{th} \tag{8}$$

Here, c_1 and c_2 represent the average capacity per UE for AP#1 and AP#2, respectively. Also, c_{th} represents an arbitrary threshold value. On the other hand, if the following formula is satisfied, the AP to which the optical cell (p, q) belongs is changed (i.e. the optical ID to be broadcast is changed).

$$|c_1 - c_2| > c_{th} \tag{9}$$

The method of selecting optical cell (p, q) is described in detail in the next section. The UEs in optical cell (p, q) receives the changed optical ID and connect to the specified AP.

TABLE 1. Notation for optical cell control.

Variable	Definition
c_1, c_2	Capacity per UE under AP#1 or AP#2
c_1', c_2'	Capacity per UE under AP#1 or AP#2 (value in previous loop)
c_{th}	Threshold of capacity difference per UE
(m, l)	Previously controlled optical cell coordinates
(p, q)	Optical cell coordinates to be controlled
M	Number of optical cells deployed in the horizontal direction
L	Number of optical cells deployed in the vertical direction
Ω	Total number of optical cells
ω	Total number of optical cells attributed to AP#1
δ	Identification number of the optical cell attributed to AP#1
τ	Identification number of the optical cell attributed to AP#2
d_δ^{12}	Distance between the optical cell belonging to AP#1 (identification number δ) and AP#2
d_τ^{21}	Distance between the optical cell belonging to AP#2 (identification number τ) and AP#1
$(a_\varepsilon, b_\varepsilon)$	Optical cell coordinates of identification number ε

C. OPTICAL CELL CONTROL ALGORITHM

Changing the optical cell selection order for determining which AP the optical cell belongs to, will significantly change the overall network capacity. This is because the capacity is affected by the modulation and coding scheme (MCS) chosen to suit the different RSSI values which depend on the distance between the optical cell and the AP [35]. Therefore, we introduce an optical cell selection algorithm that considers the physical distance between the optical cell and the AP. Two algorithms, ScanLine-based and MinDist-based, are presented; the notations for ScanLine-based and Min Dist-based are given in Table 1.

Figure 6 shows a graphical representation of ScanLine-based. In ScanLine-based, optical cells are selected in raster scan manner. As an example, we consider the case that the distribution of UEs fluctuates from the equilibrium state in Fig. 5(a) and the capacity of each UE changes. When the distribution of UEs changes, the AP allocation of optical cells is changed from the initial cell allocation in the central equilibrium shown in Fig. 5(a) according to the cases $c_1 - c_2 > 0$ or $c_1 - c_2 < 0$, respectively. Here, the initial state varies depending on AP placement. In the initial state, each optical cell is assigned to the AP with the smallest distance.

In the situation where $c_1 - c_2 > 0$, as shown in Fig. 6(a), the optical cells belonging to AP#2 are reassigned to AP#1

Algorithm 1 ScanLine-Based

Require: $(m, l), c_1', c_2', c_1, c_2$
Ensure: (p, q)

if $|c_1 - c_2| > c_{th}$
  if $c_1 - c_2 > 0$
    if $c_1' - c_2' < 0$
      stop cell operation
    else
      if $l = 1$ **then**
  if $m = 1$ **then**
        stop cell operation
      else
        $p \Leftarrow m-1,\ q \Leftarrow$ L
      end if
    else
      $p \Leftarrow$ m, $q \Leftarrow l-1$
    end if
  else
    if $c_1' - c_2' > 0$ **then**
      stop cell operation
    else
      if $m =$ M **then**
        if $l =$ L **then**
          stop cell operation
        else
          $p \Leftarrow m+1, q \Leftarrow 1$
        end if
      else
        $p \Leftarrow m, q \Leftarrow l+1$
      end if
    end if
  end if
return (p, q)

Algorithm 2 MinDist-Based

Require: c_1', c_2', c_1, c_2
Ensure: (p, q)

if $|c_1 - c_2| > c_{th}$ **then**
  if $c_1 - c_2 > 0$ **then**
    if $c_1' - c_2' < 0$ **then**
      stop cell operation
    else
      $\varepsilon \Leftarrow \text{argmin}\left(d_\tau^{21}\right)$ for $\tau\ \{\tau \in 1, 2, \cdots, (\Omega - \omega)\}$
      $p \Leftarrow a_\varepsilon,\ q \Leftarrow b_\varepsilon$
  end if
  else
    if $c_1' - c_2' > 0$ **then**
      stop cell operation
    else
      $\varepsilon \Leftarrow \text{argmin}\left(d_\delta^{12}\right)$ for $\delta\ \{\delta \in 1, 2, \cdots, \omega\}$
      $p \Leftarrow a_\varepsilon,\ q \Leftarrow b_\varepsilon$
    end if
  end if
return (p, q)

in order from optical cell (3,5). On the other hand, in the situation where $c_1 - c_2 < 0$, as shown in Fig. 6(b), the optical cells belonging to AP#1 are reassigned to AP#2 in order from optical cell (4, 1). Optical cells are reassigned until the condition of equation (6) is satisfied.

The other approach, Min Dist-based, is shown in Fig. 7. The optical cells to be changed are determined by considering the distance between optical cell centers and AP#1 or AP#2. When $c_1 - c_2 > 0$, as shown in Fig. 7(a), among the optical cells belonging to AP#2, the optical cells with the shortest distance between the optical cell center and AP#1 (i.e. d_τ^{21}) are reassigned to AP#1 in decreasing order of distance.

On the other hand, when $c_1 - c_2 < 0$, as shown in Fig. 7(b), among the optical cells belonging to AP#1, the optical cells with the shortest distance between the optical cell center and AP#2 (i.e. d_δ^{12}) are reassigned to AP#2 in decreasing order of distance. Optical cell reassignment is repeated until equation (6) is satisfied.

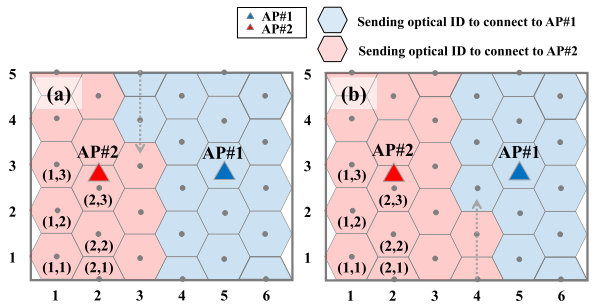

FIGURE 6. Optical cell control using ScanLine-based algorithm. (a) Optical cell operation in the situation of $c_1 - c_2 > 0$. (b) Optical cell operation in the situation of $c_1 - c_2 < 0$.

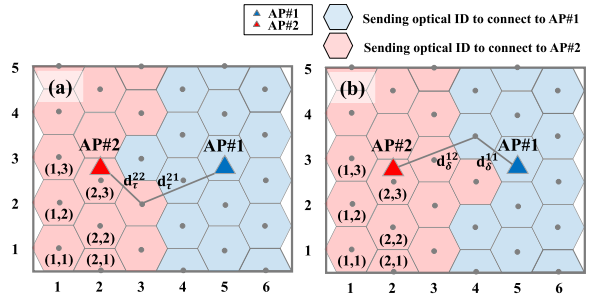

FIGURE 7. Optical cell control using MinDist-based algorithm. (a) Optical cell operation in the situation of $c_1 - c_2 > 0$. (b) Optical cell operation in the situation of $c_1 - c_2 < 0$.

IV. EVALUATION

A. EVALUATION OF OPTICAL ID TRANSMISSION AND RECEPTION

We implemented and evaluated the transmission and reception of optical IDs using commercial IoT lighting as the transmitter and an illuminance sensor as a receiver.

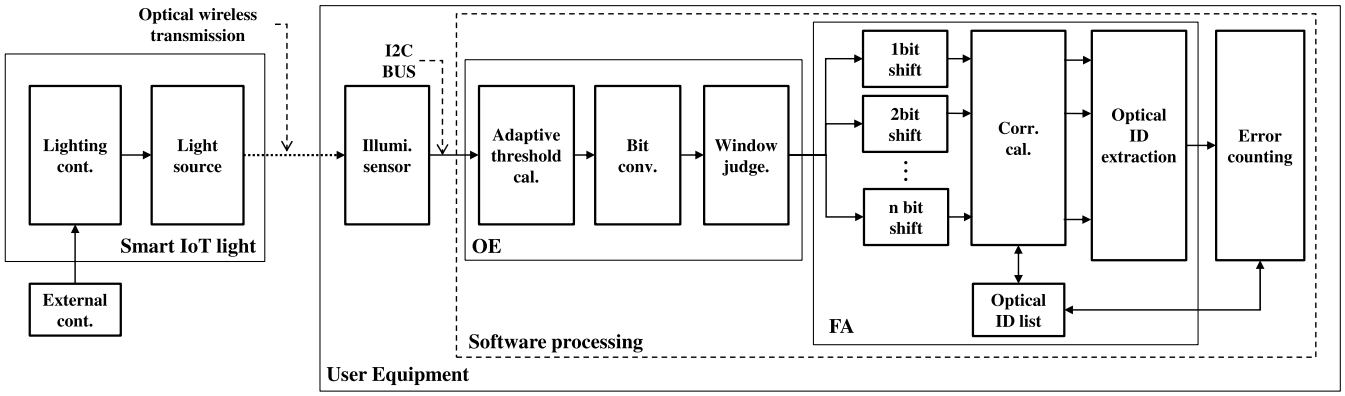

FIGURE 8. Implementation of the optical ID transmission and reception scheme.

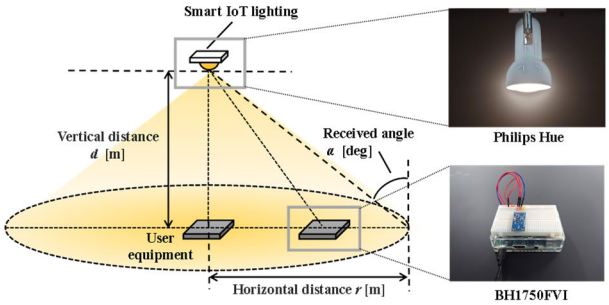

FIGURE 9. Experimental layout of light source and UE equipment for evaluation.

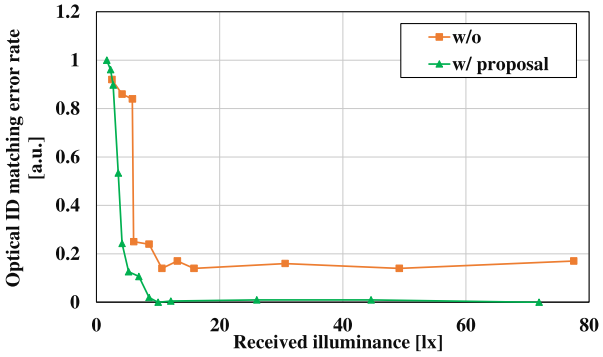

FIGURE 10. Optical ID matching error rate using proposal.

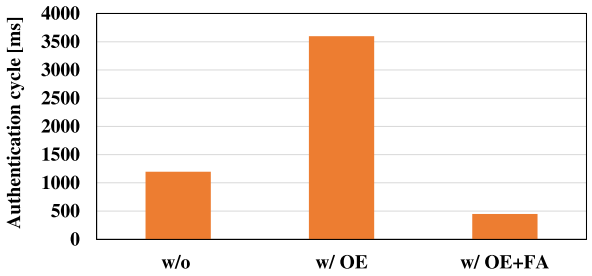

FIGURE 11. Authentication cycle reduction by using fast authentication scheme.

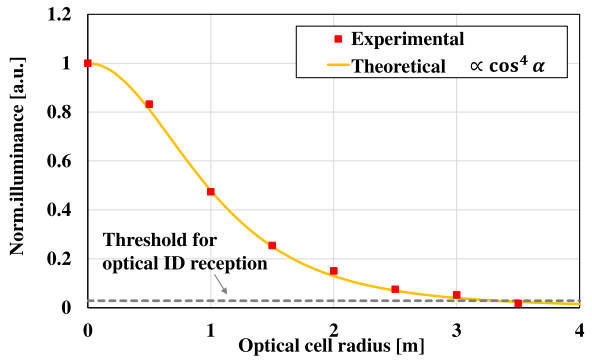

FIGURE 12. Relationship between optical cell radius and normalized illuminance of smart IoT lighting.

Figure 8 shows the processing blocks of each component. We utilized the commercial Philips Hue as smart IoT lighting hardware. Intel NUC (Linux PC) was used as the external IoT lighting controller. Moreover, an optical module (GY-30) equipped with illuminance sensor integrated circuit (IC) (BH1750FVI) was used on the receiver side. GY-30 was connected to Raspberry Pi 3B+ (representing the UE) by inter-integrated circuit (I2C) communication. The smart IoT lighting consisted of a lighting controller and light source. The lighting controller was externally driven, and optical ID was transmitted from the lighting controller to the light source. The light source emitted the n-bit ($n = 8$) optical ID as a modulation signal with the visually imperceptible optical modulation factor of 7 % [36]. The optical ID, "11000101", was repeatedly transmitted at the slow bitrate of 2.2 bps. Here, the optical ID took the form of an orthogonal bit sequence. The UE was placed 1.5 m below the light source. The illuminance sensor captured the optical wireless transmission. Here, the sampling cycle of the illuminance sensor was set to 150 ms. The signal is oversampled with $K = 3$. By using the received illuminance values, the average value was calculated for each N-bit ($N = 24$) sliding window, and 1/0 bit conversion was performed using the average value as a threshold. Window-based judgement was performed on the bit-converted signal, and an 8-bit optical ID was estimated. The optical ID was bit-shifted and a cyclic matrix was generated. Correlation was performed using the columns of the

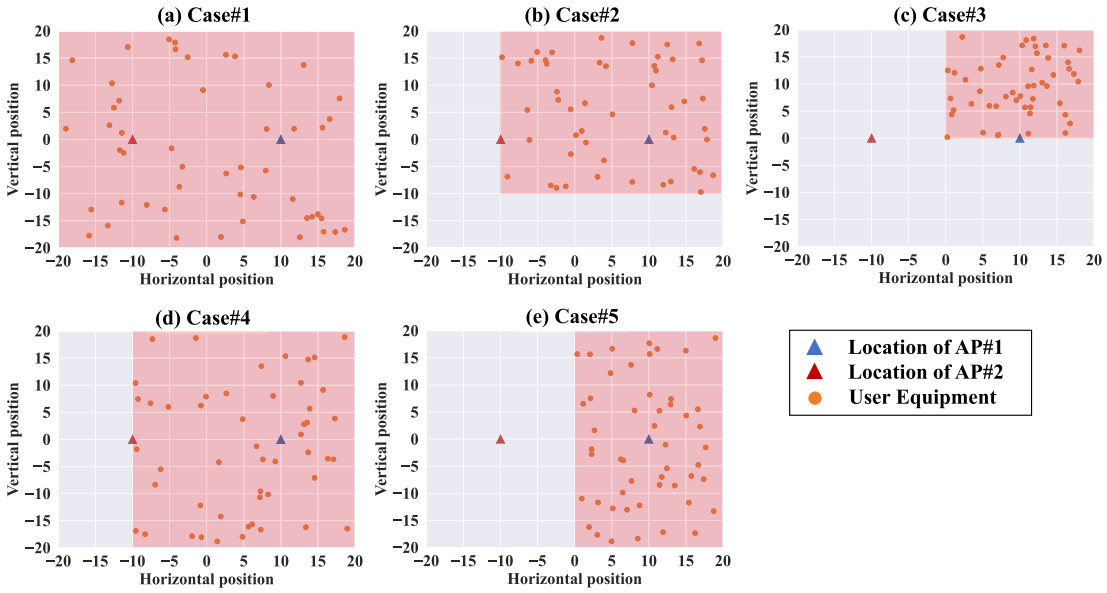

FIGURE 13. Example of UE distribution for scenario-based evaluation.

generated cyclic matrix and the columns of the optical ID list. Finally, the reference ID corresponding to the estimated optical ID was extracted.

Figure 9 shows the evaluation setup of the light source and UE. Smart IoT lighting height was set to $d = 1.5$ m. Fig. 10 shows the dependency of the optical ID reception error rate on the received illuminance level. This level is defined as the value obtained by subtracting the background illuminance from the measured illuminance sensor value. Here, the background illuminance is 226.67 lx. The existing method that uses optical correlation reception is shown as w/o. It permits reception error even if the received light illuminance is high. The error rate increased as the received illuminance fell under 16 lx. On the other hand, it is clear that our proposal, OE, reduced the error rate. OE error rate increased as the received illuminance level fell under 8.5 lx. It can be clearly understood that the proposed method can expand the acceptable range of received illuminance level while reducing the error rate compared with the existing method.

Figure 11 quantifies the reduction in authentication cycle duration. For w/o, the duration is 1200 ms (8-bit $\times$ 150 ms). In the case of w/OE, the duration is 3600 ms (24-bit $\times$ 150 ms) because of its 3 times upsampling. As shown in Fig.10, the error rate can be reduced, but the time required for pattern detection is extended. However, by introducing FA, authentication can be realized on a 3-sample cycle, so that the duration is just 450 ms (3-bit $\times$ 150 ms). Therefore, the authentication cycle can be reduced by 87.5 % compared to w/OE, and by 62.5 % compared to w/o. These results confirm that the combined use of the OE and FA proposals reduces the authentication cycle while maintaining low error rates.

Figure 12 plots the relationship between the optical cell radius (horizontal distance r) and the normalized irradiance

TABLE 2. Parameters for evaluation.

Parameters	Set value
Wireless service area	40 m × 40 m
Number of UEs	50
UE distribution function	Random model
Coordinates of AP#1	(10, 0)
Coordinates of AP#2	(-10, 0)
Wireless system	802.11 n
Frequency	2.4 GHz
Bandwidth	40 MHz
Spatial Stream	3
Propagation model	Site-general models (ITU-R P.1238-7)
MCS	Active
Optical cell radius	From 1 m to 10 m
Capacity difference threshold value c_{th}	1 Mbps

of the smart IoT lighting. It can be seen that the illuminance characteristic of the IoT lighting used in this study is proportional to $\cos^4\alpha$ (where $\alpha = \tan^{-1}(d/r)$). Based on the fact that the recommended illuminance for a typical office is 300 lx or more, the threshold illuminance of 8.5 lx, where the error rate increases with the "w/proposal" shown in Fig. 10, is plotted as a dashed line. From this result, if a light source offering the illuminance of 300 lx at $d = 1.5$ m and $r = 0$ m is deployed, transmission and reception of optical ID can be realized with a modulation level of 7 % or less within an optical cell radius of $r = 3.3$ m, even if there are external disturbances such as natural light or other illumination sources.

B. LOAD BALANCING EFFECT OF OPTICAL CELL CONTROL ALGORITHM

In order to evaluate the effectiveness of the proposed method in countering UE distribution fluctuations, we evaluated

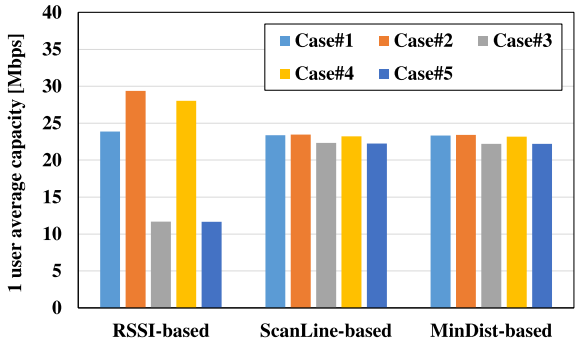

FIGURE 14. Comparison of average capacity per UE in Case#1-5.

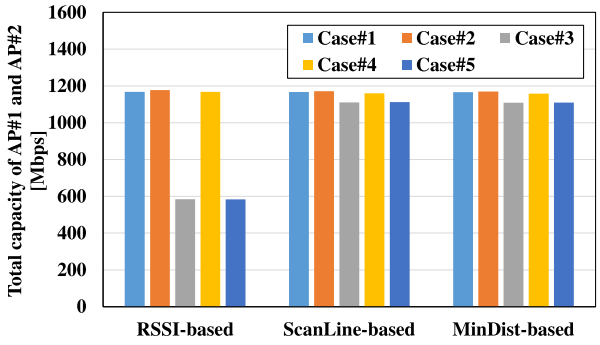

FIGURE 16. Comparison of the total capacity of AP#1 and AP#2 in Case#1-5.

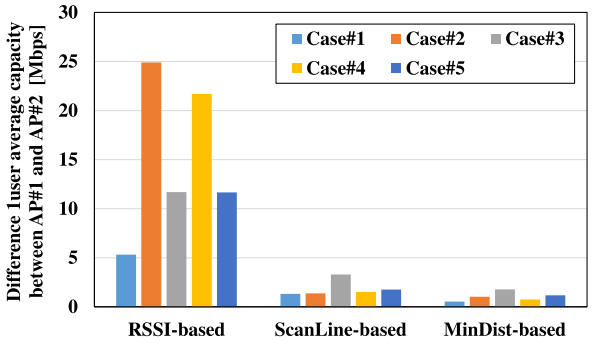

FIGURE 15. Comparison of the difference in average capacity per UE between AP#1 and AP#2 in Case#1-5.

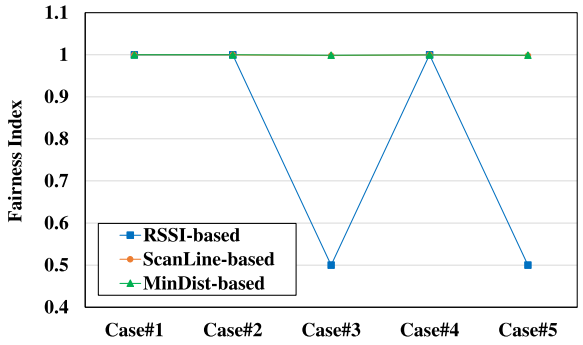

FIGURE 17. Fairness Index between AP#1 and AP#2 in Case#1-5.

several scenarios. Table 2 shows the evaluation parameters. AP#1 and AP#2 were deployed in a space of 40 m × 40 m. 50 UEs were arranged within the wireless service area. We used site-general models so propagation followed the ITU model [37]. UEs were assumed to be randomly distributed within a region. As an example, optical cell radius was set to 2 m. The capacity difference threshold, c_{th}, was set to 1 Mbps.

In evaluating the proposal, we considered five scenarios. Figure 13 shows the UE distribution in five scenarios. Case#1: UEs were distributed throughout the wireless service area. That is, Case#1 represents uniform user distribution. Case#3 concentrates all users into the first quadrant. Case#2 represents an intermediate state between Case#1 and Case#3. On the other hand, Case#5 represents a case where all users are concentrated in first and fourth quadrant. Case#4 represents an intermediate state between Case#1 and Case#5. Cases#3 and Case5# are examples of the extreme distribution concentration in which all UEs concentrate on AP#1as controlled by RSSI. To benchmark the proposal, we also evaluated a conventional RSSI-based scheme that determines the connection based on the strength of RSSI.

Figure 14 shows the average capacity per UE for Case#1-5. Looking at RSSI-based, we can see a significant capacity decrease in Case#3 and Case#5. This is because the connections are concentrated on one AP due to the extreme bias in the distribution of UEs. On the other hand, ScanLine-based and MinDist-based maintained a capacity of at least 20 Mbps in all cases. In particular, stable capacity was obtained even in the situations of Case#3 and Case#5.

Figure 15 shows the difference in average capacity per UE between AP#1 and AP#2 for Case#1-5. RSSI-based yields extreme differences in Case#2-5. In particular, in Case#2 and Case#4, it can be seen from Fig. 15 that the difference in average capacity per UE exceeds 20 Mbps. In addition, there is a difference exceeding 10 Mbps in Case#3 and Case#5. On the other hand, ScanLine-based and MinDist-based reduced the difference to within 3 Mbps in all cases, with MinDist-based offering the smallest throughput difference. Here, the capacity difference increases according to the set value of c_{th} (i.e. capacity difference threshold). If c_{th} is set extremely small, the capacity difference may not converge within the set value stochastically. This depends on the number of UEs in the optical cell that should be controlled. Reducing the optical cell radius, stochastically reduces the number of UEs existing in the target optical cell. This makes it possible to reduce the average capacity difference.

Figure 16 shows the total capacity of AP#1 and AP#2. RSSI-based reduces the total capacity in Case#3 and Case#5. It can be said that the decrease in capacity is caused by the extreme bias in UE distribution. On the other hand, ScanLine-based and MinDist-based have slightly reduced total capacity in Case#3 and Case#5. However, they are superior to RSSI-based. This is because the UE is intentionally connected to an AP with a small RSSI to avoid concentration on one AP. Here, the capacity of the UE depends on the RSSI. This is because the MCS changes the modulation scheme according

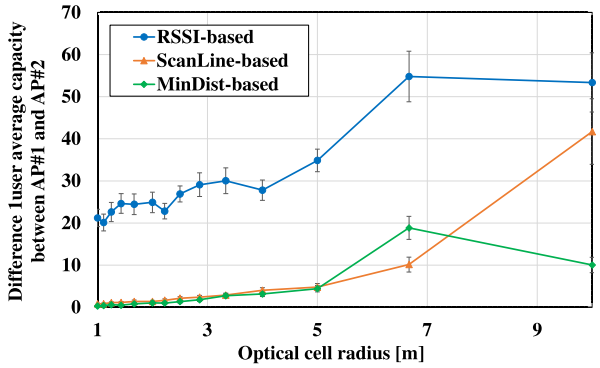

FIGURE 18. Optical cell size dependence of the difference of UE capacity between AP#1 and AP#2 in Case#2.

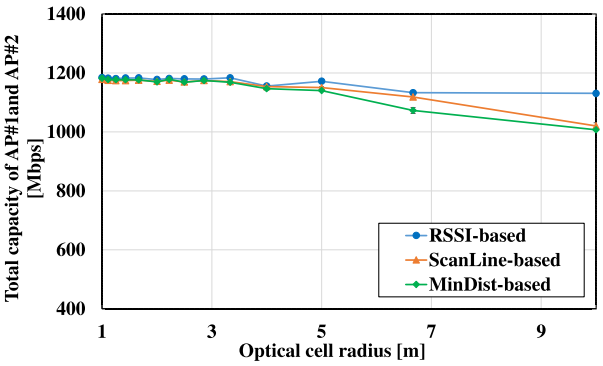

FIGURE 19. The relationship between optical cell size and the total capacity of AP#1 and AP#2 in Case#2.

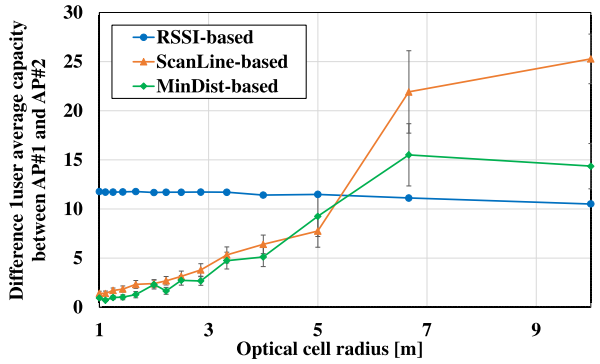

FIGURE 20. Optical cell size dependence of the difference of UE capacity between AP#1 and AP#2 in Case#3.

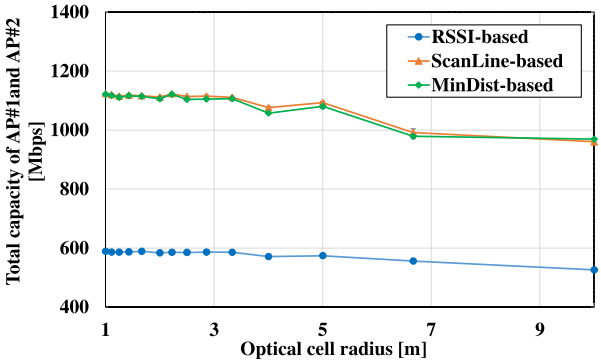

FIGURE 21. The relationship between optical cell size and the total capacity of AP#1 and AP#2 in scenario Case#3.

to RSSI. In other words, UE capacity is reduced by intentionally connecting it to an AP with a small RSSI. However, in the proposal, the reduction in capacity is suppressed as much as possible by strategically selecting the optical cell to be offloaded in consideration of the positional relationship of the optical cell center and the AP.

Figure 17 shows the Fairness Index between AP#1 and AP #2. With reference to the results in Fig. 16, RSSI-based suffered a drop in Fairness Index in Case#3 and Case#5. However, ScanLine-based and MinDist-based offered improved fairness compared to RSSI-based. In particular, MinDist-based attained better Fairness Index values than ScanLine-based. Even if the wireless system frequency is changed to 5GHz, as long as each AP covers the wireless service area, the total capacity fluctuates slightly, but it does not significantly affect the results of the fairness index.

C. OPTICAL CELL SIZE DESIGN

The design of the overlaid optical cell size is considered to be a parameter that affects the communication capacity and the difference among UEs. Therefore, we evaluated the difference in UE capacity and overall capacity as a function of optical cell size. Here, optical cell radius ranged from 1 m to 10 m. Among the five scenarios shown in Fig. 13, Case#2 and Case#3 with biased UE distribution were shown as examples. A random UE distribution was generated for the configurations of Case#2 and Case#3. The number of trials was set to 100, and the average value was calculated.

Figure 18 shows the optical cell size dependency of the average capacity difference per UE between AP#1 and AP#2 in Case#2. The legend shows the RSSI-based, ScanLine-based, and MinDist-based values. The 95 % confidence interval is also added. Under the condition of relatively large optical cell radius, all methods have a large average capacity difference per UE between AP#1 and AP#2. This is because the number of UEs under one optical cell is stochastically large, and the destination APs of many UEs are changed at the same time. On the other hand, with relatively small optical cell radius, the number of UEs under one optical cell is stochastically small, so the destination APs of only a small number of UEs are changed at the same time. Therefore, by reducing the optical cell radius, more fine-grained control can be achieved. Although RSSI-based shows a limited improvement in the average capacity difference per UE, ScanLine-based and MinDist-based offer a significant reduction in the average capacity difference per UE. Fig. 19 shows the relationship between optical cell size and the total capacity of AP#1 and AP#2 in Case#2. With relatively large optical cell radius, all methods suffer a drop in total capacity. This can be attributed to the coarse granularity of the connection control. On the other hand, it can be seen that the total capacity is improved by decreasing the optical cell radius.

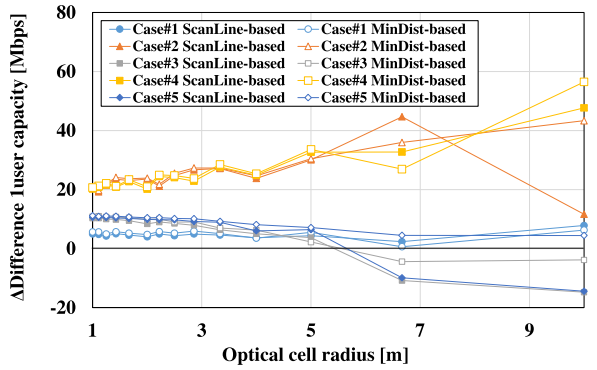

FIGURE 22. The comparison result with RSSI-based in the difference of UE capacity between AP#1 and AP#2 for all scenario.

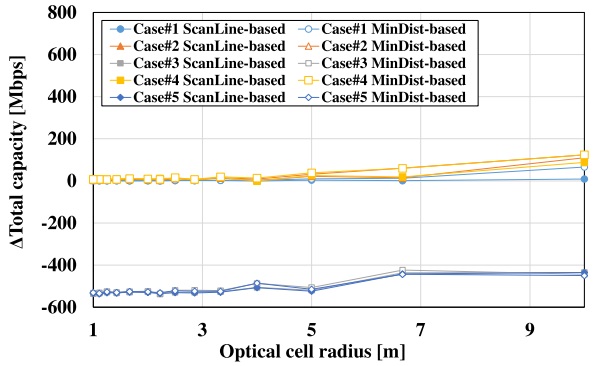

FIGURE 23. The comparison result with RSSI-based in the total capacity between AP#1 and AP#2 for all scenario.

Figures 20 and Fig. 21 show the average capacity difference per UE and the total capacity of AP#1 and AP#2 in the extreme UE distribution scenario of Case#3. In Case#3, UE distribution is more concentrated than in Case#2, and all UEs are assigned to AP#1 with RSSI-based. However, ScanLine- based and MinDist-based force the UEs in some optical cells to connect to AP#2, which has a lower RSSI, thereby preventing all UEs from connecting to AP#1. Fig. 20 shows that RSSI-based does not reduce the average capacity difference per UE, even if the optical cell radius is reduced. This is due to the fact that all UEs are attributed to AP#1. On the other hands, ScanLine-based and MinDist-based improve the average capacity difference compared to RSSI-based, with the demarcation point around 5 m. In addition, by further reducing the optical cell radius, the capacity difference is further improved with ScanLine-based and MinDist-based. These results show that using more fine-grained optical cell control, using our ScanLine-based and MinDist-based methods, enables fair wireless connections between APs. As can be seen from Fig. 21, it is shown that the total capacity of RSSI-based is smaller than that of ScanLine-based and MinDist-based. This is also due to the fact that all UEs were biased towards AP#1, as described in Fig. 20. It can be clearly seen that the total capacity is improved by reducing the optical cell radius with ScanLine-based and MinDist-based.

Figures 22 and 23 summarize the comparison of RSSI-based and proposal in Case#1-5. Fig. 22 shows the results of the capacity difference per user between AP#1 and AP#2 in ScanLine-based and MinDist-based compared to RSSI-based. The vertical axis, Δ difference 1user capacity, represents the absolute difference between the RSSI-based 1user average capacity and the ScanLine-based/MinDist-based 1user average capacity. In other words, it means that the proposed method has superior performance in the region where Δ difference 1user capacity is a positive value (i.e. the capacity difference per user can be reduced compared to RSSI-based). From Fig. 22, with optical cell radius of 5 m or less, the proposal reduced the capacity difference per user compared to the RSSI-based in all scenarios.

Figure 23 shows the total capacity of ScanLine-based and MinDist-based compared to RSSI-based. The vertical axis Δ total capacity represents the absolute difference between the average total capacity of RSSI-based minus the average total capacity of ScanLine-based/MinDist-based. In other words, in the region where Δ total capacity is negative, the proposed method improves the total capacity compared with RSSI-based. From Fig. 23, it is understood that the improvement in total capacity by the proposed method is remarkable in Case#3 and Case#5 as compared with the other cases. In the other cases, RSSI-based has higher total capacity. However, by reducing the optical cell radius, the difference in total capacity between the RSSI-based and the proposal becomes smaller. At 5 m or less, use of the proposed method suppresses the deterioration to just a few several percent of the expected maximum total capacity.

These results indicate that by making the optical cell smaller, the average capacity difference per user can be reduced and total capacity can be improved. A reduction in optical cell size means a stochastic decrease in the number of UEs existing in the optical cell. Therefore, by making the optical cell smaller, we approach personal connection control for each UE. Depending on cell size, the proposed method is closer to the case of trying to acquire the individual position of the user as in related research. As already mentioned, many methods for grasping UE position have been studied and are advancing day by day. However, for highly accurate position estimation, it is necessary to attach a new device to the UE or modify the UE [25]–[28]. In contrast, our proposal does not specifically need to collect the location of the UE itself. It also allows location-based control without changing UE/AP or adding devices on the wireless system side. Since RSSI-based location awareness is utilized in [22], the RSSI map is formed in the AP based on the RSSI of the signal received from the UE. The relative position of the UE determines the connection to the AP. However, since [22] collects only the position relative to the AP, it offers inadequate connection control according to the area, which is one of the goals of our system. (i.e., flexibly constructing a wireless connection restriction area or connectable area within the wireless service area) Furthermore, another originality of our proposal is the optical

cell control algorithm. In our algorithm, the optical cell that offers less capacity reduction is selected from among many optical cells in consideration of the positional relationship between the optical cell center and the APs. Strategic optical cell control that also takes into account the optical cell radius reduces the average capacity difference per user while reducing the capacity deterioration in extremely biased user distribution scenarios.

It is also important to note that there is a trade-off between the granularity of equipment placement and performance improvement. It is necessary to design optical cell radius that take into account the cost of equipment and the performance improvement from each perspective.

V. CONCLUSION

We proposed a novel wireless control architecture that applies optical wireless to the control plane of WLAN systems. To reduce the deployment barrier, we proposed a software-based optical ID transmission and reception scheme using consumer-based smart IoT lighting and the illumination sensors widely implemented in smartphones. Experiments confirmed that the proposed OE algorithm reduces the error rate compared to the existing optical correlation-based receiving scheme, while the FA algorithm can shorten the authentication cycle, which is a challenge when using OE. The results of the experiments showed that the combined use of OE and FA can reduce the authentication cycle by 62.5 % (1200 ms to 450 ms) and reduce the error rate compared to existing methods.

Furthermore, we also proposed two optical cell control algorithms (i.e. ScanLine-based and MinDist-based) to guarantee high network quality against temporal variations in UE location density. Compared to the existing RSSI-based scheme, our proposals showed improvements in terms of average per-user capacity difference and fairness among APs, while maintaining the total capacity in several highly-skewed UE distribution scenarios. In addition, for optical cell design, an evaluation against optical cell radius was performed. It was shown that the average per-user capacity difference between APs and the overall capacity are improved as the optical cell radius is reduced. In particular, the optical cell radius of 5 m was found to be the threshold for improving the average capacity difference per user. Since there is a trade-off between installation granularity and the resulting performance improvement, it is necessary to deploy optical cells considering each aspect.

REFERENCES

[1] "Cisco visual networking index: Forecast and trends, 2017–2022," Cisco, San Jose, CA, USA, Nov. 2018.

[2] M. Seufert, C. Moldovan, V. Burger, and T. HoBfeld, "Applicability and limitations of a simple WiFi hotspot model for cities," in *Proc. 13th Int. Conf. Netw. Service Manage. (CNSM)*, Tokyo, Japan, Nov. 2017, pp. 1–7.

[3] A. Reyes-Menendez, P. R. Palos-Sanchez, J. R. Saura, and F. Martin-Velicia, "Understanding the influence of wireless communications and Wi-Fi access on customer loyalty: A behavioral model system," *Wireless Commun. Mobile Comput.*, vol. 2018, pp. 1–16, Dec. 2018.

[4] W. S. Lee, J. Moon, and M. Song, "Attributes of the coffee shop business related to customer satisfaction," *J. Foodservice Bus. Res.*, vol. 21, no. 6, pp. 628–641, Oct. 2018.

[5] N. Masri, F. I. Anuar, and A. Yulia, "Influence of Wi-Fi service quality towards tourists' satisfaction and dissemination of tourism experience," *J. Tourism, Hospitality Culinary Arts*, vol. 9, no. 2, pp. 383–397, Oct. 2017.

[6] J. Jeon, M. Yoo, and N. Christodoulidou, "The impact of Wi-Fi service on millennial diners," *J. Hospitality Tourism Technol.*, vol. 10, no. 3, pp. 383–400, Sep. 2019.

[7] W. Sun, O. Lee, Y. Shin, S. Kim, C. Yang, H. Kim, and S. Choi, "Wi-Fi could be much more," *IEEE Commun. Mag.*, vol. 52, no. 11, pp. 22–29, Nov. 2014.

[8] H. Luo, "A secure server-paid hot spot Wi-Fi internet service method," in *Proc. IEEE 6th Circuits Syst. Symp. Emerg. Technol., Frontiers Mobile Wireless Commun.*, Shanghai, China, May 2004, pp. 1–12.

[9] H. Tang, L. Yang, J. Dong, Z. Ou, Y. Cui, and J. Wu, "Throughput optimization via association control in wireless LANs," *Mobile Netw. Appl.*, vol. 21, no. 3, pp. 453–466, Jun. 2016.

[10] Z. Zhang, X. Di, J. Tian, and Z. Zhu, "A multi-objective WLAN planning method," in *Proc. Int. Conf. Inf. Netw. (ICOIN)*, Da Nang, Vietnam, 2017, pp. 86–91.

[11] F. Cao, Z. Zhong, Z. Fan, M. Sooriyabandara, S. Armour, and A. Ganesh, "User association for load balancing with uneven user distribution in IEEE 802.11ax networks," in *Proc. 13th IEEE Annu. Consum. Commun. Netw. Conf. (CCNC)*, Las Vegas, NV, USA, Jan. 2016, pp. 487–490.

[12] A. Mishra, M. Shin, and W. Arbaugh, "An empirical analysis of the IEEE 802.11 MAC layer handoff process," *ACM Comput. Commun. Rev.*, vol. 33, no. 2, pp. 93–102, Apr. 2003.

[13] H. Kobayashi, E. Kameda, Y. Terashima, and N. Shinomiya, "Towards sustainable heterogeneous wireless networks: A decision strategy for AP selection with dynamic graphs," *Comput. Netw.*, vol. 132, pp. 99–107, Feb. 2018.

[14] S. Han, M. Kim, B. Lee, and S. Kang, "Directional handoff using geomagnetic sensor in indoor WLANs," in *Proc. IEEE Int. Conf. Pervas. Comput. Commun.*, Mar. 2012, pp. 128–134.

[15] Z. Zhi, J. Wu, X. Meng, M. Yao, Q. Hu, and Z. Tang, "AP deployment optimization in non-uniform service areas: A genetic algorithm approach," in *Proc. IEEE 90th Veh. Technol. Conf. (VTC-Fall)*, Honolulu, HI, USA, Sep. 2019, pp. 1–5.

[16] Y. Jian, Y. Liu, S. K. Venkateswaran, D. M. Blough, and R. Sivakumar, "A quantitative exploration of access point mobility for mmWave WiFi networks," in *Proc. IEEE Int. Conf. Commun. (ICC)*, Dublin, Ireland, Jun. 2020, pp. 1–7.

[17] Y. Bejerano and S.-J. Han, "Cell breathing techniques for load balancing in wireless LANs," *IEEE Trans. Mobile Comput.*, vol. 8, no. 6, pp. 735–749, Jun. 2009.

[18] S. Suherman, S. Andoni, and A. H. Rambe, "Clustered beacon signal cell breathing for load balancing in mobile and wireless networks," in *Proc. 3rd Int. Conf. Electr., Telecommun. Comput. Eng. (ELTICOM)*, Sep. 2019, pp. 13–16.

[19] H. Velayos, V. Aleo, and G. Karlsson, "Load balancing in overlapping wireless LAN cells," in *Proc. IEEE Int. Conf. Commun.*, Paris, France, Jun. 2004, pp. 3833–3836.

[20] U. Shafi, M. Zeeshan, N. Iqbal, N. Kalsoom, and R. Mumtaz, "An optimal distributed algorithm for best AP selection and load balancing in WiFi," in *Proc. 15th Int. Conf. Smart Cities, Improving Qual. Life Using ICT IoT (HONET-ICT)*, Islamabad, Pakistan, Oct. 2018, pp. 65–69.

[21] D. G. Narayan, R. Nivedita, S. Kiran, and M. Uma, "Congestion adaptive multipath routing protocol for multi-radio wireless mesh networks," in *Proc. Int. Conf. Radar, Commun. Comput. (ICRCC)*, Tiruvannamalai, India, Dec. 2012, pp. 72–76.

[22] H. C. Yu, K. Alhazmi, and R. R. Rao, "Wi-Fi roaming as a location-based service," in *Proc. IEEE Int. Conf. Commun. (ICC)*, Dublin, Ireland, Jun. 2020, pp. 1–7.

[23] Z. Han, T. Lei, Z. Lu, X. Wen, W. Zheng, and L. Guo, "Artificial intelligence-based handoff management for dense WLANs: A deep reinforcement learning approach," *IEEE Access*, vol. 7, pp. 31688–31701, 2019.

[24] Y. Zheng, Y. Chen, X. Xie, and W.-Y. Ma, "GeoLife2.0: A location-based social networking service," in *Proc. 10th Int. Conf. Mobile Data Manage., Syst., Services Middleware*, Taipei, Taiwan, 2009, pp. 357–358.

[25] L. W. J. Tsay, T. Shiigi, Z. Huang, X. Zhao, T. Suzuki, Y. Ogawa, and N. Kondo, "Temperature-compensated spread spectrum sound-based local positioning system for greenhouse operations," *IoT*, vol. 1, no. 2, pp. 147–160, Sep. 2020.
[26] J. Qi and G.-P. Liu, "A robust high-accuracy ultrasound indoor positioning system based on a wireless sensor network," *Sensors*, vol. 17, no. 11, p. 2554, Nov. 2017.
[27] A. Sobehy, E. Renault, and P. Muhlethaler, "NDR: Noise and dimensionality reduction of CSI for indoor positioning using deep learning," in *Proc. IEEE Global Commun. Conf. (GLOBECOM)*, Waikoloa, HI, USA, Dec. 2019, pp. 1–6.
[28] X. Wang, L. Gao, S. Mao, and S. Pandey, "DeepFi: Deep learning for indoor fingerprinting using channel state information," in *Proc. IEEE Wireless Commun. Netw. Conf. (WCNC)*, New Orleans, LO, USA, Mar. 2015, pp. 1666–1671.
[29] M. Castro, A. J. Jara, and A. F. G. Skarmeta, "Smart lighting solutions for smart cities," in *Proc. 27th Int. Conf. Adv. Inf. Netw. Appl. Workshops*, Barcelona, Spain, Mar. 2013, pp. 1374–1379.
[30] P. Smallwood, "Lighting, LEDs and smart lighting market overview," presented at the U.S. Dept. Energy SSL Workshop, Raleigh, NC, USA, 2016.
[31] I. Chew, D. Karunatilaka, C. P. Tan, and V. Kalavally, "Smart lighting: The way forward? Reviewing the past to shape the future," *Energy Buildings*, vol. 149, pp. 180–191, Aug. 2017.
[32] A. M. Al-Ghaili, H. Kasim, N. M. Al-Hada, M. Othman, and M. A. Saleh, "A review: Buildings energy savings–lighting systems performance," *IEEE Access*, vol. 8, pp. 76108–76119, 2020.
[33] L. I. Albraheem, L. H. Alhudaithy, A. A. Aljaser, M. R. Aldhafian, and G. M. Bahliwah, "Toward designing a Li-Fi-based hierarchical IoT architecture," *IEEE Access*, vol. 6, pp. 40811–40825, 2018.
[34] M. Miki, K. Yoshida, M. Yoshimi, H. Ito, and M. Nagano, "Faster illuminance convergence for the intelligent lighting system using visible light communication," in *Proc. IEEE Int. Conf. Syst., Man, Cybern. (SMC)*, Oct. 2012, pp. 3179–3184.
[35] V. Jones and H. Sampath, "Emerging technologies for WLAN," *IEEE Commun. Mag.*, vol. 53, no. 3, pp. 141–149, Mar. 2015.
[36] J. J. Koenderink and A. J. van Doorn, "Visibility of unpredictably flickering lights," *J. Opt. Soc. Amer.*, vol. 64, no. 11, pp. 1517–1522, Nov. 1974.
[37] P. Series, *Propagation Data and Prediction Methods for the Planning of Indoor Radio Communication Systems and Radio Local Area Networks in the Frequency Range 300 MHz to 100 GHz*, document Rec. ITU-R P.1238-8, 2015.

RYOTA SHIINA received the M.E. degree in material science and engineering from Tokyo Institute of Technology, Tokyo, Japan, in 2014. In 2014, he joined the NTT Access Network Service Systems Laboratories, where he has been engaged in research on optical access systems mainly related to optical video distribution systems, optical radio-over-fiber transmission systems, and optical wireless communication systems. He is a member of IEICE. He received the Young Researcher's Award from the Institute of Electronics, Information, and Communication Engineers (IEICE) of Japan, in 2018, and the Encouraging Award from IEICE Technical Committee on Communication Systems (CS), in 2017.

SHINYA TAMAKI received the B.A. degree in physics from the International Christian University, Tokyo, Japan, in 2005, and the M.E. degree in precision engineering from The University of Tokyo, Tokyo, in 2009. In 2009, he joined the NTT Access Network Service Systems Laboratories, where he was involved in research and development of next-generation optical access systems. His current research interests include system architecture of edge computing and the Internet of Things, including virtualization, orchestration, and provisioning.

KAZUTAKA HARA received the B.S. degree in applied physics from Tokyo University of Science, Japan, in 2003, and the M.E. degree in applied physics and the Ph.D. degree in engineering from Tokyo Institute of Technology, Japan, in 2005 and 2011, respectively. In 2005, he joined the NTT Access Network Service Systems Laboratories, Yokosuka, Kanagawa, Japan, where he engaged in research on nonlinear optical transmission systems. Since 2007, he has been in charge of research on ten gigabit-class high-speed TDM access systems. From 2011 to 2014, he worked on software development and server operation of Video On Demand (VOD) services at NTT Plala. He is currently with the NTT Access Network Service Systems Laboratories. His current interests include high performance transmission systems and architectural design for the vision of the future access networks. He is a member of the Institute of Electronics, Information, and Communication Engineers (IEICE) of Japan. He was a recipient of the Best Paper Award at the OptoElectronics and Communications Conference (OECC) 2010 and at the International Conference on Optical Internet (COIN) 2010, respectively.

TOMOHIRO TANIGUCHI received the B.E. and M.E. degrees in precision engineering from The University of Tokyo, Tokyo, Japan, in 2000 and 2002, respectively, and the Ph.D. degree in electrical, electronic and information engineering from Osaka University, Osaka, Japan, in 2010. In 2002, he joined the NTT Access Network Service Systems Laboratories, where he has been engaged in research on optical access systems mainly related to optical heterodyne technologies, radio-on-fiber transmission, and video distribution systems.

SHUNSUKE SARUWATARI (Member, IEEE) received the B.E. degree from The University of Electro-Communications, Japan, in 2002, and the M.S. and Ph.D. degrees from The University of Tokyo, Japan, in 2004 and 2007, respectively. In 2007, he was a Visiting Researcher at Illinois Genetic Algorithms Laboratory, University of Illinois at Urbana-Champaign. From 2008 to 2011, he was a Research Associate with the Research Center for Advanced Science and Technology, The University of Tokyo. From 2012 to 2015, he was a tenure-track Assistant Professor with the Graduate School of Informatics, Shizuoka University, Japan. He is currently an Associate Professor with the Graduate School of Information Science and Technology, Osaka University, Japan. His research interests include wireless networks, sensor networks, and system software. He is a member of ACM, IPSJ, and IEICE.

TAKASHI WATANABE (Member, IEEE) received the B.E., M.E., and Ph.D. degrees from Osaka University, Japan, in 1982, 1984, and 1987, respectively. He joined the Faculty of Engineering, Tokushima University, in 1987, and moved to the Faculty of Engineering, Shizuoka University, in 1990. He was a Visiting Researcher with the University of California, Irvine, from 1995 to 1996. He has been a Professor with the Graduate School of Information Science and Technology, Osaka University, since 2013. His research interests include mobile networking, *ad-hoc* sensor networks, the IoT/M2M networks, and intelligent transport systems, specially MAC and routing. He is a member of IPSJ and IEICE. He has served on many program committees for networking conferences, IEEE, ACM, IPSJ, and IEICE.